Pion-kaon femtoscopy in Pb-Pb collisions at $\sqrt{s_{NN}} = 2.76$ TeV modeled in (3+1)D hydrodynamics coupled to the Therminator 2 code, and the effect of delayed kaon emission

Adam Kisiel*

Faculty of Physics, Warsaw University of Technology, ul. Koszykowa 75, PL-00662 Warsaw, Poland

(Received 19 April 2018; published 30 October 2018)

Nonidentical particle femtoscopy measures the size of the system emitting particles ("radius") in heavy-ion collisions as well as the difference between mean emission space-time coordinates of two particle species ("emission asymmetry"). The system created in such collisions at the CERN Large Hadron Collider behaves collectively and its dynamics is well described by hydrodynamic models. A significant emission asymmetry between pions and kaons, coming from collective flow, enhanced by contribution from flowing resonances is predicted. Calculations within the (3+1)D viscous hydrodynamic model coupled to statistical hadronization code Therminator 2, corresponding to Pb-Pb collisions at $\sqrt{s_{NN}} = 2.76$ TeV, are presented. Femtoscopic radii and emission asymmetry for pion-kaon pairs as a function of collision centrality are obtained. The radii grow linearly with cube root of particle multiplicity density. The emission asymmetry is negative and comparable to the radius, indicating that pions are emitted closer to the center of the system and/or later than kaons. Recent ALICE Collaboration measurements of identical kaon femtoscopy shows that kaons are emitted, on average, 2.1 fm/c later than pions. The calculation is modified by introducing such delay. The system source size is only weakly affected. In contrast the pion-kaon emission asymmetry is directly sensitive to such delays and the modified calculation shows significantly lower values of asymmetry. This is an argument that the measurement of the pion-kaon femtoscopic correlation function is a sensitive probe of time delays in particle emission.

DOI: 10.1103/PhysRevC.98.044909

I. INTRODUCTION

The system created in collisions of heavy-ions at ultra-relativistic energies is dynamically expanding and cooling. In the early stages of the evolution it is thought to be in a deconfined phase (the quark-gluon plasma), where the matter behaves as a strongly coupled liquid with small specific viscosity [1–4]. Models which employ hydrodynamic equations to describe this behavior are successful in reproducing many of the observables in such collisions. The most common are the transverse momentum spectra and elliptic flow, which are also modified by event-by-event fluctuations. This behavior of the system in momentum space is driven by space-time characteristics of the source: its size and gradients in pressure. Therefore, the correct description of the momentum space observables must be accompanied by a proper simulation of its space-time structure and its dynamics. The basic principles of such a description were established at the BNL Relativistic Heavy Ion Collider (RHIC) [5,6]. They were then applied at the CERN Large Hadron Collider (LHC) [7–11] to describe the data on identical particle femtoscopy [12–15]. The important features include significant prethermal flows, an equation of state that does not include a first-order phase transition, a careful treatment of strongly decaying resonances, introduction of hadron interactions post-freeze-out, as well as possible addition of viscosity.

The femtoscopic radii obtained from identical pion analysis agree well with model calculations [14], indicating that the dynamics of the system at the LHC is well described. Similar data for kaons show novel features [15]. The femtoscopic radii for kaons are larger than expected from the naive "m_T scaling" argument. The radii are also larger than predicted by the Therminator 2 model, which includes hydrodynamic evolution of the system followed by the statistical hadronization. A second calculation presented in [15] is based on a hydrodynamical model coupled to the hadronic rescattering code [11] and is able to reproduce the larger values of the kaon radii. The increase is attributed to the delay of the emission time of kaons, coming from the rescattering via the K^* meson. Experimental analysis with the theoretical formalism proposed in [11] shows that on average kaons are emitted later than pions by 2.1 fm/c. This result is then interpreted as evidence for the extended "rescattering" phase in the evolution of the heavy-ion collision. Confirmation of the existence of such a phase has profound consequences for modeling such collisions and experimental data interpretation.

The femtoscopic technique is not limited to pairs of identical particles. For pairs of nonidentical particles, the correlation arises from the final Sstate interactions (FSIs), that is Coulomb when both particles in the pair are charged and strong interaction when both particles are hadrons. The original motivation for the formulation of the nonidentical particle femtoscopy formalism was to measure the difference in average time of the emission of various types of particles [16], which was called "emission asymmetry." It was

*kisiel@if.pw.edu.pl

later realized that spatial emission asymmetry produces an equivalent asymmetry signal [17,18]. Such spatial asymmetry arises naturally in a hydrodynamically expanding system, where thermal and flow velocities are comparable. Heavy-ion collisions produce such a system. In a detailed analysis of the nonidentical particle correlations at RHIC energies [19] the emission asymmetry between pions, kaons, and protons was studied in detail. It was found that the emission asymmetry coming from the radial flow in the system is enhanced, for pion-kaon and pion-proton pairs, by additional nontrivial effects coming from the decay of flowing resonances. A complete set of emission asymmetries for three pair types was presented. Also the formalism was introduced and its validity was tested. The results show that the same formalism should be applicable in heavy-ion collisions at the LHC.

This work contains two main results. It presents the calculation of the pion-kaon femtoscopic correlation functions for Pb-Pb collisions at the LHC energies, for selected centralities. The calculation is carried out within the model consisting of (3+1)D viscous hydrodynamics coupled to the Therminator 2 statistical hadronization, resonance propagation, and decay code. System size and emission asymmetry between pions and kaons is extracted as a function of centrality. These results can be directly compared to experimental data. In particular experimental acceptance constraints similar to those imposed by the ALICE detector are applied. In a separate calculation the model is modified to include the additional emission time delay for kaons, as suggested by the experimental data from ALICE [15]. Several values of the time delay are studied, including the 2.1 fm/c value obtained by ALICE. I explore how the introduction of time delay influences the extracted emission asymmetry and system size. I present separate sets of emission asymmetries, as a function of collision centrality, for selected values of time delay. Experimental data from ALICE can be directly compared to these datasets. The identical kaon femtoscopy results are explained by the introduction of time delay coming from regeneration of the K^* resonance in the hadronic rescattering phase. If this interpretation is correct, the same time delay must be observed in the pion-kaon emission asymmetry measurement. Such an observation would be an important and independent confirmation of the existence of the "rescattering" phase of the Pb-Pb collisions at the LHC. The pion-kaon emission asymmetry is one of the few observables with such a direct sensitivity to the effects of the rescattering phase.

The work is organized as follows. In Sec. II the model used in this work is described and the data sample which was analyzed is characterized. In Sec. III the formalism of the nonidentical particle correlations is briefly introduced. Sec. IV discusses the main results of this work: the pion-kaon femtoscopic correlation functions as well as system sizes and emission asymmetries which were extracted from their analysis.

II. (3+1)D HYDRO AND THERMINATOR 2 MODELS

The model used in this work is composed of two parts. The collective expansion is modeled in (3+1)D viscous hydrodynamics. The details of the implementation and the formalism of the model are presented in [20–22]. The particle emission is implemented in the statistical hadronization and resonance propagation and decay simulation code Therminator 2 [23].

In particular the calculations presented in this work have been intentionally performed on exactly the same generated model dataset, which was used in a previous work on identical particle femtoscopy [7] to which I contributed. These calculations were later used by the ALICE Collaboration for comparison with experimental data for identical kaon femtoscopy [15]. The discrepancies between the model calculation and data are an explicit scientific motivation for the studies in this work. The reader is referred to the works mentioned above for details of the model calculations. Here only the important features are briefly mentioned.

The viscous hydrodynamic model is used, following the second-order Israel-Stewart equations [24]. A hard equation of state is used [5,6], in particular a parametrization interpolating between lattice QCD results [25] at high temperatures and the hadron gas equation of state at low temperatures. All chemical potentials are set to zero. Smooth initial conditions are taken for the hydrodynamic evolution, given by the Glauber model. The initial time for the hydrodynamic evolution is 0.6 fm/c, viscosity coefficients are $\eta/s = 0.08$ and $\zeta/s = 0.04$, and the freeze-out temperature $T_t = 140$ MeV.

The calculation is performed for five sets of initial conditions, corresponding to impact parameter b values (in fm), for the Pb-Pb collisions at $\sqrt{s_{NN}} = 2.76$ TeV, of 3.1, 5.7, 7.4, 8.7, and 9.9 fm. They correspond, in terms of the average particle multiplicity density $\langle dN_{ch}/d\eta \rangle$, to the following centrality ranges at the LHC [26]: 0–10%, 10–20%, 20–30%, 30–40%, and 40–50%.

The Therminator 2 code [23] then performs a statistical hadronization on the freeze-out hypersurfaces obtained from the hydro model via the Cooper-Frye formalism. Chemical and kinetic freeze-outs are equated. Importantly the model does not include hadronic rescattering. It does, however, implement the propagation and decay (in cascades if necessary) of all known hadronic resonances. With these assumptions the model is able to describe a large number of observables at the RHIC and at the LHC [5,8,20,21]. The final output from the model is a set of events, each composed of final-state particles, with information on the particle identity, momentum, and space-time freeze-out coordinates provided for each of them.

III. NONIDENTICAL PARTICLE FEMTOSCOPY FORMALISM

The formalism for nonidentical particle femtoscopy is described in great detail in [18,19]. Here only the main concepts are briefly introduced.

The femtoscopic correlation function measures the conditional probability to observe two particles of a given type at a certain relative momentum $\vec{q}$.[1] In order to eliminate the trivial dependence on particle acceptance, such probability is normalized to the product of probabilities of measuring each

[1] In this work a notation is used where three-vectors are indicated with the arrow, $\vec{a}$, while four-vectors are indicated with a bold font, $\boldsymbol{a}$.

particle separately. Experimentally in heavy-ion collisions the measurement consists of constructing the distribution of pairs of particles of given types X and Y, here pions (π) and kaons (K), coming from the same event and storing their relative momenta in the distribution $A_{\pi K}(\vec{q})$. Then a similar procedure is repeated, but the two particles come from two different events, giving the reference distribution $B_{\pi K}(\vec{q})$. The correlation function is then

$$C(\vec{q}) = A_{\pi K}(\vec{q})/B_{\pi K}(\vec{q}). \quad (1)$$

For a pair consisting of a charged pion and a charged kaon, the femtoscopic correlation arises from the strong and Coulomb FSI. Currently no model of heavy-ion collisions implements such interactions, therefore it must be introduced *a posteriori* via the so-called "afterburner" procedure [19]. The pairs of particles are obtained from model events, and samples $A_{\pi K}$ and $B_{\pi K}$ are constructed in a procedure resembling the experimental one as closely as possible. However, for each model pair going into the $A_{\pi K}$ sample an additional weight corresponding to the modulus squared of the Bethe-Salpeter amplitude $\Psi_{\pi K}$ of the pair is stored [18]. The correlation function is then a ratio of the weighted $A_{\pi K}$ sample to the $B_{\pi K}$ sample. The amplitude $\Psi_{\pi K}$ is described in detail in the following section of the paper.

The procedure described above produces a correlation function with femtoscopic effects as well as all the other event-wide correlations present in the model. Some additional nonfemtoscopic correlations were studied in the previous works [27,28] and were found to be significant for pion-kaon pairs. However, it was also shown that such correlations can be efficiently corrected in the experiment with a data-driven procedure. Since this work focuses on the analysis of the femtoscopic effect, these additional correlations are not studied. Instead a modified procedure is employed, where the $B_{\pi K}$ sample is simply the $A_{\pi K}$ sample without femtoscopic weights. In such calculations the nonfemtoscopic correlations are not present [19,27].

The theoretical interpretation of the correlation function assumes that it is expressed as

$$C(\vec{k^*}) = \frac{\int S(\boldsymbol{r^*}, \vec{k^*})|\Psi_{\pi K}(\boldsymbol{r^*}, \vec{k^*})|^2 d^4\boldsymbol{r^*}}{\int S(\boldsymbol{r^*}, \vec{k^*}) d^4\boldsymbol{r^*}}, \quad (2)$$

where $\boldsymbol{r^*} = \boldsymbol{x}_1 - \boldsymbol{x}_2$ is a spatial separation between the creation points $\boldsymbol{x}_1$ and $\boldsymbol{x}_2$ of the two particles in the pair rest frame () at the moment of creation of the particle that is created later.[2] $\vec{k^*}$ is the momentum of the first particle in the PRF, so it is half of the pair relative momentum in this frame (for identical particles $\vec{q} = 2\vec{k^*}$). In this work the convention defined in [19] is followed, where the first particle in the pair is the one with smaller mass; here it is the pion. This means that negative values of "emission asymmetry" correspond to pions emitted on average later than kaons and/or closer to the center of the system. S is the source emission function and can be interpreted as a probability of emitting a given particle pair from a given set of emission points with given momenta.

For a charged-pion–charged-kaon, pair $\Psi_{\pi K}$ contains contributions from the strong and Coulomb FSI [18]. However for this particular pair type, the strong interaction is expected to be small in the region of $k^* < 150$ MeV/c, where this analysis is performed (the region of significant pion-kaon strong interaction via the K^* resonance is located around its decay momentum, that is $k^* = 289$ MeV). In this region the femtoscopic signal is dominated by the Coulomb interaction, especially for the emission asymmetry signature. Therefore in this work a simplification is used: only the Coulomb part of the interaction is considered. It is done self-consistently first to calculate the model correlation functions and later in the fitting procedure to extract the system size and emission asymmetry. With this modification,

$$\Psi_{\pi K} = \sqrt{A_C(\eta)}[e^{-ik^*r^*}F(-i\eta, 1, i\xi)], \quad (3)$$

where $\eta = 1/(k^* a_C)$, $A_C = 2\pi\eta[\exp(2\pi\eta) - 1]^{-1}$ is the Gamow factor, $\xi = k^* r^*(1 + \cos\theta^*)$, and F is the confluent hypergeometric function. θ^* is the angle between $\vec{k^*}$ and $\vec{r^*}$ and a_C is the Bohr radius which is equal to ± 248.52 fm for the like-sign (unlike-sign) pion-kaon pair. The correlation function then shows a positive correlation effect for unlike-sign pion-kaon pairs and a negative correlation effect for like-sign pairs. This $\Psi_{\pi K}$ is used as a basis to calculate the weight for the model correlation function calculation and in the fitting procedure.

The "afterburner" weighting procedure, as described above, is used to calculate the femtoscopic correlation functions for all charge combinations of charged-pion–charged-kaon pairs. The functions are stored in the spherical harmonics representation [29]. Only two components of this representation are analyzed: the $l = 0$, $m = 0$ and the real part of the $l = 1$, $m = 1$. It was shown in [19] that these two components contain the relevant signals for the system size and emission asymmetry. The pions and kaons were selected in the p_T range of 0.15 to 2.5 GeV/c and pseudorapidity range $|\eta| < 1.0$, which corresponds to the reconstruction and particle-identification (PID) acceptance of the ALICE detector. Two example correlation functions, one for like-sign and another for unlike-sign pion-kaon pairs, are shown in Fig. 1. A positive (negative) correlation effect, coming from the Coulomb attraction (repulsion) for unlike-sign (like-sign) pion-kaon pairs, can be clearly seen. Similarly, Re C_1^1 clearly deviates from zero, indicating a nonzero emission asymmetry between pions and kaons, discussed in the following section.

A. Origins of asymmetry

Space-time separation $\boldsymbol{r}^*$ in PRF, as defined here, only has the spatial component. The interaction is also naturally described in PRF. The "emission asymmetry" between pions and kaons is this separation averaged over all pion-kaon pairs. In principle the analysis could be carried out in PRF. In this case it would measure the asymmetry directly in PRF. However, PRF is by definition different for every pair. The value of asymmetry in this frame is difficult to interpret. In contrast,

[2]Both $\boldsymbol{k^*}$ and $\boldsymbol{r^*}$ are four-vectors; however, since the identities of the particles and therefore their masses are given, only three components of $\boldsymbol{k^*}$ are independent, therefore the three-vector notation for $\vec{k^*}$ is used throughout this work.

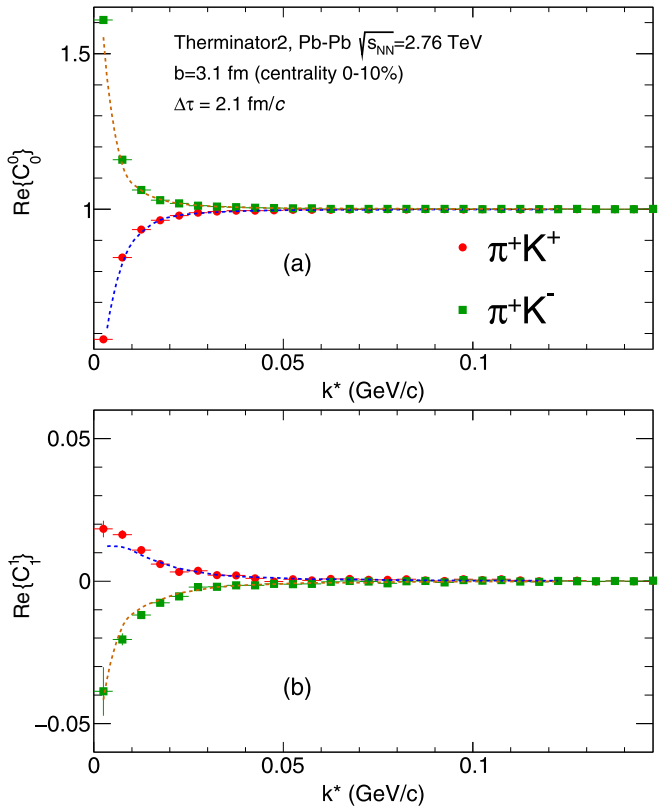

FIG. 1. Spherical harmonics components: real part of C_0^0 in panel (a) and real part of C_1^1 in panel (b), of the example charged pion-charged kaon femtoscopic correlation function calculated in the (3+1)D hydrodynamic model coupled to Therminator 2 code for central Pb-Pb collisions at $\sqrt{s_{NN}} = 2.76$ TeV. Lines show the fit to the correlation function (see text for details).

three-dimensional femtoscopy of pions and kaons in ultrarelativistic heavy-ion collisions is routinely carried out in the longitudinally comoving system (LCMS), defined as a frame where the component of the total momentum of the pair along the beam axis vanishes. Following Bertsch-Pratt [30] the three axes in LCMS are defined as follows: "longitudinal" or "long" along the beam axis, "outwards" or "out" along the pair total momentum in the plane perpendicular to the beam axis (the "transverse" plane), and "sideward" or "side" perpendicular to the other two. LCMS was proposed as a frame more suitable for femtoscopic measurements, as it can be viewed as being connected to the frame where the fluid element emitting the two particles is at rest. The theoretical interpretation of the source parameters in LCMS is then more straightforward. For pion-kaon emission asymmetry LCMS has another unique property. In a collider setup for a collision of identical ions, such as the Pb-Pb collisions at the LHC measured in a detector like ALICE, the symmetry considerations require that the emission asymmetry vanishes in the longitudinal and sidewards directions. Only the "out" asymmetry is allowed to be nonzero. The "emission asymmetry" is then described by a single fitting parameter in the experimental analysis, instead of three. It should be stressed that the formalism itself is sensitive to all three components of the asymmetry, and would able to measure all three of them simultaneously if they were nonzero. In fact in experimental analysis the measurement of the "side" and "long" asymmetry is always performed simultaneously with the "out" asymmetry. So far all measurements have indeed observed zero asymmetry in these two directions, as expected.

It is argued above that important physics is contained in the emission asymmetry in LCMS, specifically in the nonvanishing "out" component. The asymmetry in PRF has no time component; however, the Lorentz transformation from PRF to LCMS results in nonzero time asymmetry in LCMS. The femtoscopic correlation function has, as its variable, the relative momentum, which only has three independent components, so it is possible to measure only three components of the asymmetry. Two of them ("side" and "long") are vanishing due to symmetry reasons given above. Therefore, in LCMS, the measured "out" asymmetry is a convolution of the "time" and "space" asymmetry. The relation between the "out" relative separation in PRF, $r^*_{\rm out}$, the space separation in "out," $r_{\rm out} = x^\pi_{\rm out} - x^K_{\rm out}$, and time separation $\Delta t = t^\pi - t^K$ in LCMS for a given pair is [19]

$$r^*_{\rm out} = \gamma_t (r_{\rm out} - \beta_t \Delta t), \tag{4}$$

where β_t is the pair transverse velocity and γ_t is the corresponding Lorentz factor. The "emission asymmetry" is then $\langle r^*_{\rm out} \rangle$, where averaging is done over all pairs. When the averaging is done in LCMS, the asymmetry will have two components: the "space" and "time" asymmetries with a possible nontrivial correlation between them. In LCMS a nonzero "space" asymmetry in the "out" direction can be interpreted in the following way: one particle species (e.g., pions) is, on average, emitted closer to (further from) the center of the source than the other particle species (e.g., kaons). With the convention used in this work where pions are always taken as the first particle in the pair, a negative asymmetry means that pions are emitted closer to the center of the source. Similarly a nonzero "time" asymmetry is interpreted as indicating that one particle species is, on average, emitted earlier or later than the other particle species. However the minus sign in Eq. (4) means that within the same convention negative emission asymmetry may indicate that pions are, on average, emitted later than kaons. The formalism itself measures only a single value for the asymmetry and it is unable to distinguish between the two types. In conclusion, a negative emission asymmetry may mean that pions are emitted closer to the center than kaons, or that pions are emitted later than kaons, or some combination of both. It is also possible that pions are emitted further from the center of the system than kaons (which gives positive emission asymmetry), but are also emitted so much later than kaons that the time difference shifts the asymmetry back to negative values. This inherent ambiguity in the asymmetry measurement is explicitly addressed in this work, where possible origins of both space and time asymmetries are investigated and their expected relative magnitudes are discussed.

The formalism itself does not impose any limitations on the value or the sign of emission asymmetry. However, the radial flow mechanism, which is a fundamental ingredient of the hydrodynamic description of the heavy-ion collision

at the LHC naturally produces emission asymmetry between particles of different mass. Radial flow results in significant "space" asymmetry in LCMS, where pions are emitted closer to the center of the system than kaons. This asymmetry is significantly enhanced if pions and kaons are also produced from the decays of flowing resonances. A detailed discussion of this effect is given in [19]. In short, there is a qualitative difference in the way that resonance decays influence the emission pattern of pions and kaons. The pion decay momentum for most common resonances is similar to or larger than a pion mass. The direction of the velocity of such pions is heavily randomized, and is no longer strongly influenced by the flow field. As a result the average emission point of pions from resonances is close to the geometrical center of the source. In contrast for kaons the decay momentum is usually small compared to the kaon mass. The parent resonance is usually quite heavy, therefore it is strongly pushed by the flow field. After decay the kaon velocity direction is still strongly correlated with the parent one. Therefore the average emission point for kaons is strongly pushed by the flow to the edge of the source, producing a large emission asymmetry with respect to pions. In addition the decay of resonances occurs with a delay with respect to the "primordial" particle creation. Pions are relatively more frequently produced from resonances than kaons. This introduces another, "time" component of the asymmetry, where pions are emitted later than kaons. Please note that according to Eq. (4) both effects produce a negative contribution to the emission asymmetry, so the resulting pion-kaon emission asymmetry is strongly negative. The relative contributions of both effects have also been estimated in [19], showing that the asymmetry that can be attributed to flow is dominant.

The calculation in [19] as well as simulations in this work both use the Therminator model, which does not include the hadronic rescattering phase. The theoretical interpretation of the kaon femtoscopy results from ALICE [15] states that, in addition to all the effects described above, there is an additional time delay of kaon emission coming from the constant regeneration of the K^* resonance in the rescattering phase. This effect is not included in the calculations mentioned above. It contributes to the pion-kaon emission asymmetry with an opposite sign to both the "space" component coming from flow and the "time" delay from resonance decay. These nontrivial dependencies are explored in this work.

B. Correlation function fitting

The model correlation function is analyzed in a procedure closely resembling an experimental one. First it is assumed that the source is an ellipsoid with a Gaussian density profile. It has different widths in three directions defined in LCMS. From the symmetry of the heavy-ion collision it is expected that the emission asymmetry between particles arises only in the "out" direction [17–19]. Its magnitude is another model parameter. The final form of the assumed emission function is then

$$S(\vec{r}) \approx \exp\left(-\frac{[r_{\text{out}}-\mu_{\text{out}}]^2}{2\sigma_{\text{out}}^2}-\frac{r_{\text{side}}^2}{2\sigma_{\text{side}}^2}-\frac{r_{\text{long}}^2}{2\sigma_{\text{long}}^2}\right), \quad (5)$$

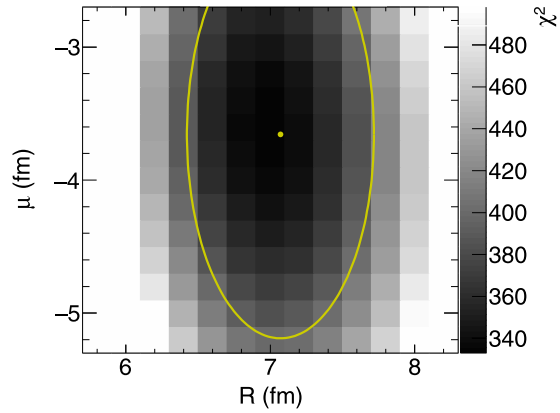

FIG. 2. Example of the χ^2 values obtained in the fitting procedure for one of the pion-kaon femtoscopic correlation functions (see text for details). The point shows the best-fit value, the ellipse is a 1σ contour.

where σ are the sizes of the system in the three directions and μ is the emission asymmetry. The correlation function for nonidentical particles is only weakly sensitive to the details of the three-dimensional shape of S. Such details were much more precisely studied through identical particle femtoscopy [12–15]. Therefore, here the number of independent fitting parameters is minimized by fixing $\sigma_{\text{side}} = \sigma_{\text{out}}$ and $\sigma_{\text{long}} = 1.3\sigma_{\text{out}}$. The values of the scaling coefficients are based on corresponding values of system sizes from identical pion femtoscopy [14]. In this work the focus is the emission asymmetry, which is not accessible in the identical femtoscopy technique. As a result only two independent fit parameters remain: σ_{out} characterizing the overall system size as well as μ_{out} containing information of the pion-kaon emission asymmetry.

For a given set of σ_{out} and μ_{out} values, forming a rectangular lattice of points, a "fit" correlation function is calculated according to Eq. (2) with Ψ given by Eq. (3). Then a χ^2 value is calculated between this function and the "experimental-like" one calculated for Therminator 2 data. The calculation is repeated for all combinations of σ_{out} and μ_{out} values in predefined ranges. An example result of such a calculation—the values of χ^2 for each lattice point—is shown in Fig. 2. The minimization procedure is then employed to find the σ_{out} and μ_{out} values that minimize the χ^2 value. This set is the result of the fit, shown in the figure as a point (best-fit value) and an ellipse (1σ contour). The procedure is implemented in the CorrFit software [31]. The fitting procedure also accounts for the so-called "purity" of the sample, or the percentage of the pairs that form the Gaussian core of the system. The values for this purity parameter depend mostly on the percentages of pions and kaons that come from strongly decaying resonances. Their abundances depend on the temperature of the chemical freeze-out. This temperature is very similar for RHIC and LHC calculations in Therminator, therefore in this work the values estimated in the previous work for RHIC [19] are used. The χ^2 landscape shown in Fig. 2 also reveals very small correlation between the σ_{out} and μ_{out} fitting results. This has

been observed consistently for all performed fits. It indicates that uncertainties of σ_{out} and μ_{out} are uncorrelated.

IV. RESULTS

In this work the femtoscopic correlation for all four charge combinations of the pion-kaon pair, π^+K^+, π^+K^-, π^-K^+, and π^-K^-, are calculated. All correlations are fitted independently. At the end the results of the fitting procedure—the radii and emission asymmetries—are averaged between all four pair charge combinations. The calculation has been performed for the event samples obtained from the (3+1)D hydrodynamic code coupled to the Therminator 2 statistical hadronization, resonance propagation, and decay code. The five samples used correspond to Pb-Pb collisions at the selected centralities. In the figures data for the five samples are plotted at the corresponding $\langle dN_{ch}/d\eta\rangle^{1/3}$.

The standard calculation is performed on the generated events directly. Following the experimental insight [15], calculations with a specific modification are also done. For each kaon its emission time is altered by adding a delay $\Delta\tau$, distributed according to a Gaussian, with a certain width and mean. First a calculation with a mean time delay of 2.1 fm/c and a width of 2 fm/c was performed. Then three other calculations were done, one with the mean changed to 1 fm/c, next with the mean changed to 3.2 fm/c, and the last one with the width changed to 0.3 fm/c. The results of the fits to all the calculated correlation functions are presented in Fig. 3. The emission asymmetry seems to be sensitive only to the mean value of the time shift. The width of the Gaussian does not seem to matter. Also the fact that due to long Gaussian tails some kaons would actually receive a negative delay (so in fact they will be emitted earlier than in standard simulation) does not seem to influence the emission asymmetry.

The figure shows the set of predictions for the pion-kaon source size and asymmetry in heavy-ion collisions at the LHC energy. The system size grows with event multiplicity; the dependence is to a good approximation linear. This is expected and understood, as similar increase has been consistently observed in all measurements for identical pion femtoscopy. The pion-kaon system size is a convolution of the size of the system emitting pions and kaons at a given velocity. Therefore, it is mostly influenced by the source radius that is larger, which usually is the one for pions.

The emission asymmetry in the default calculation is universally negative. This means that pions are emitted closer to the center of the system and/or later than kaons. This emission asymmetry is relatively large, comparable to the system size. It was shown in [19] that it is coming from the spatial asymmetry produced by a flow of primordial pions and kaons, further enhanced by the effects of flowing resonances, as described in Sec. III A. The randomization of pion momenta from resonance decays—the key element of the discussion above—is a core component of the resonance propagation and decay process and is fully implemented in all Therminator 2 simulations, including the ones which reproduce elliptic flow values for all particles [21].

Whenever a time delay is introduced for kaons, the fit results are visibly changed. The overall system size is only slightly affected. It grows by approximately 0.5 fm for all calculations. The increase is larger when the introduced time delay is larger. The width of the time delay distribution has a smaller but still visible effect on size. The calculation with a time delay distribution width of 0.3 fm/c gives a size about 0.1–0.2 fm smaller than the calculation with the time delay width of 2 fm/c.

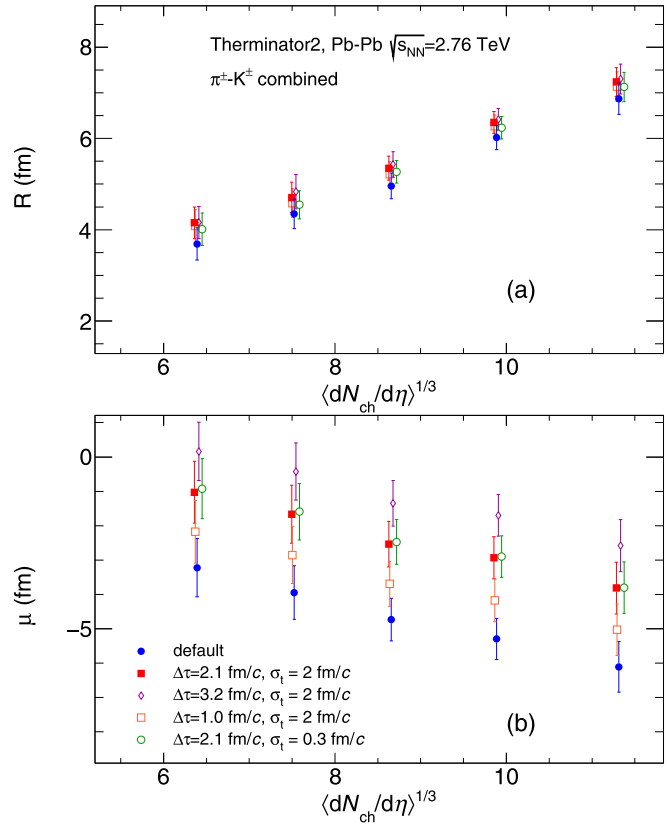

FIG. 3. Source size (a) and pion-kaon emission asymmetry (b) from pion-kaon correlation functions calculated in the Therminator 2 model for Pb-Pb collisions at $\sqrt{s_{NN}} = 2.76$ TeV for selected centralities. Blue solid circles show the default calculation. Red solid squares, orange open squares, green open circles, and violet open diamonds show calculations with selected values of additional time delay for kaons (see text for details). Some points were shifted slightly in the x direction for clarity.

The kaon emission time delay has a direct and strong effect on the pion-kaon emission asymmetry. As expected, the delay significantly decreases the emission asymmetry. When the time delay is increased to 3.2 fm the emission asymmetry even turns positive for most peripheral collisions. The value of introduced time delay is shifting the extracted emission asymmetry and the value of this shift is independent of centrality (and therefore system size).

In Fig. 4 the difference in the extracted emission asymmetry between the default calculation and the calculations with the kaon emission time delay is plotted as a function of the value of this introduced delay. The dependence between the two seems to be a direct one-to-one correspondence, independent of the system size. In other words this calculation shows that pion-kaon emission asymmetry is directly and

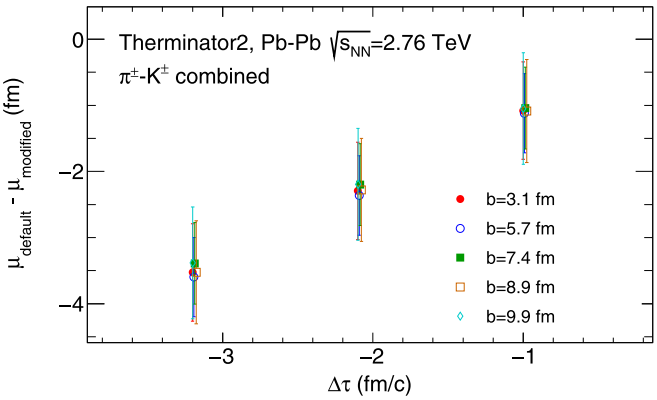

FIG. 4. The difference in the extracted pion-kaon emission asymmetry between the default calculation for the Therminator 2 model for Pb-Pb collisions at $\sqrt{s_{NN}} = 2.76$ TeV and the calculations with additional kaon emission time delay, plotted as a function of the value of additional shift. Some points were shifted slightly in the x direction for clarity.

linearly sensitive to any delays in emission time of kaons. The calculation shows that the experimental measurement of the pion-kaon emission asymmetry can be a very sensitive cross-check of the model interpretation of identical pion and kaon femtoscopy data given in [15]. In particular, if the interpretation given in this work is correct, than ALICE should observe pion-kaon emission asymmetry of approximately −4 fm in most central collisions, instead of −6 fm predicted by the default Therminator 2 calculation. In other words, the "default" calculation in this work presents a "null" hypothesis, without the effects of hadronic rescattering. It should be then compared with a full simulation, with hadronic rescattering effects included, which is beyond the scope of this work. The hadronic rescattering is in itself a very complicated procedure with many processes taking place at the same time. It may often be difficult to identify, which of those many contributions are the important ones. In this work I identify such contributions: the emission time delays. In this sense this works enables a more focused study of the future full simulations with hadronic rescattering phase present.

It should be noted that the analysis of the kaon emission time presented in [15] are given for central events only. It is postulated that the emission delay is a result of rescattering via the K^* resonance. If that is the case (and given that the chemical freeze-out temperature and consequently the relative abundance of this resonance changes little with centrality), then the value of the delay should be similar at other centralities too. This work shows the predictions for them as well. On the other hand if the experimentally observed asymmetry will be different at other centralities, the calculations shown in Fig. 3 can be used to estimate the kaon emission time delay from the data.

V. SUMMARY

This work presents the first calculations of pion-kaon femtoscopic correlation functions for Pb–Pb collisions at $\sqrt{s_{NN}} =$ 2.76 TeV at selected collision centralities. System size and emission asymmetry were extracted for each pion-kaon charge combination and collision centrality separately. The extracted system size is observed to linearly increase with the cube root of the charged particle multiplicity density. The emission asymmetry is large and negative, indicating that pions are emitted closer to the center of the source and/or later than kaons. Such asymmetry is naturally expected in a hydrodynamically flowing medium, where a large fraction of particles are produced via resonance decay. The results are also qualitatively consistent with the calculations at top RHIC collision energies.

Following the experimental results for identical kaon femtoscopy, the calculation has been modified by introducing an emission time delay for kaons. The pion-kaon asymmetry is shown to be directly and linearly sensitive to such delay. The introduction of a time delay of 2.1 fm reduces the pion-kaon asymmetry to approximately −4 fm for central collisions, compared to approximately −6 fm for the default calculation. Such a difference should be measurable in the ALICE experiment. The experimental data on pion-kaon emission asymmetry can be a direct and sensitive test of the existence of emission time delay for kaons. The confirmation of its existence would be a strong and independent argument for the importance of the hadronic rescattering phase at the LHC.

ACKNOWLEDGMENT

This work has been supported by the Polish National Science Centre under Grant No. UMO-2014/13/B/ST2/04054.

[1] J. Adams *et al.* (STAR Collaboration), Nucl. Phys. A **757**, 102 (2005).
[2] K. Adcox *et al.* (PHENIX Collaboration), Nucl. Phys. A **757**, 184 (2005).
[3] B. B. Back *et al.*, Nucl. Phys. A **757**, 28 (2005).
[4] I. Arsene *et al.* (BRAHMS Collaboration), Nucl. Phys. A **757**, 1 (2005).
[5] W. Broniowski, M. Chojnacki, W. Florkowski, and A. Kisiel, Phys. Rev. Lett. **101**, 022301 (2008).
[6] S. Pratt, Nucl. Phys. A **830**, 51c (2009).
[7] A. Kisiel, M. Gałażyn, and P. Bożek, Phys. Rev. C **90**, 064914 (2014).
[8] P. Bożek, Phys. Rev. C **95**, 054909 (2017).
[9] I. A. Karpenko, Y. Sinyukov, and K. Werner, Phys. Rev. C **87**, 024914 (2013).
[10] I. A. Karpenko and Yu. M. Sinyukov, Phys. Rev. C **81**, 054903 (2010).
[11] V. M. Shapoval, P. Braun-Munzinger, I. A. Karpenko, and Yu. M. Sinyukov, Nucl. Phys. A **929**, 1 (2014).
[12] K. Aamodt *et al.* (ALICE Collaboration), Phys. Lett. B **696**, 328 (2011).
[13] J. Adam *et al.* (ALICE Collaboration), Phys. Rev. C **92**, 054908 (2015).

[14] J. Adam *et al.* (ALICE Collaboration), Phys. Rev. C **93**, 024905 (2016).
[15] S. Acharya *et al.* (ALICE Collaboration), Phys. Rev. C **96**, 064613 (2017).
[16] R. Lednicky, V. L. Lyuboshits, B. Erazmus, and D. Nouais, Phys. Lett. B **373**, 30 (1996).
[17] R. Lednicky, presented at the International Workshop on the Physics of the Quark Gluon Plasma, Palaiseau, France, September 4–7, 2001 (unpublished), arXiv:nucl-th/0112011.
[18] R. Lednicky, Phys. Part. Nucl. **40**, 307 (2009).
[19] A. Kisiel, Phys. Rev. C **81**, 064906 (2010).
[20] P. Bożek, Phys. Rev. C **85**, 034901 (2012).
[21] P. Bożek and I. Wyskiel-Piekarska, Phys. Rev. C **85**, 064915 (2012).
[22] P. Bożek, Phys. Rev. C **89**, 044904 (2014).
[23] M. Chojnacki, A. Kisiel, W. Florkowski, and W. Broniowski, Comput. Phys. Commun. **183**, 746 (2012).
[24] C. Gale, S. Jeon, B. Schenke, P. Tribedy, and R. Venugopalan, Phys. Rev. Lett. **110**, 012302 (2013).
[25] S. Borsanyi *et al.*, J. High Energy Phys. 11 (2010) 077.
[26] K. Aamodt *et al.* (ALICE Collaboration), Phys. Rev. Lett. **106**, 032301 (2011).
[27] A. Kisiel, Acta Phys. Pol. B **48**, 717 (2017).
[28] Ł. K. Graczykowski, A. Kisiel, M. A. Janik, and P. Karczmarczyk, Acta Phys. Pol. B **45**, 1993 (2014).
[29] A. Kisiel and D. A. Brown, Phys. Rev. C **80**, 064911 (2009).
[30] M. Herrmann and G. F. Bertsch, Phys. Rev. C **51**, 328 (1995).
[31] A. Kisiel, Nukleonika **49**, s81 (2004).